Journal of Biomolecular NMR, **13:** 101–112, 1999.
KLUWER/ESCOM

Assessing potential bias in the determination of rotational correlation times of proteins by NMR relaxation

Andrew L. Lee & A. Joshua Wand*
The Johnson Research Foundation, Department of Biochemistry & Biophysics, University of Pennsylvania, Philadelphia, PA 19104, U.S.A.

Received 18 September 1998; Accepted 21 October 1998

Key words: chemical shift anisotropy, correlation time, ^{15}N relaxation, nuclear Overhauser effect, protein NMR, spin-lattice relaxation, spin-spin relaxation

Abstract

The various factors that influence the reliable and efficient determination of the correlation time describing molecular reorientation of proteins by NMR relaxation methods are examined. Nuclear Overhauser effects, spin-lattice, and spin-spin relaxation parameters of ^{15}N NMR relaxation in ubiquitin have been determined at 17.6, 14.1, 11.7 and 9.4 Tesla. This unusually broad set of relaxation parameters has allowed the examination of the influence of chemical shift anisotropy, the functional form of the model-free spectral density, and the reliability of determined spin-spin relaxation parameters on the characterization of global tumbling of the protein. Treating the ^{15}N chemical shift anisotropy (CSA) as an adjustable parameter, a consensus value of -170 ± 15 ppm for the breadth of the chemical shift tensor and a global isotropic correlation time of 4.1 ns are found when using the model-free spectral density to fit T_1 and NOE data from all fields. The inclusion of T_2 relaxation parameters in the determination of the global correlation time results in its increase to 4.6 ns. This apparent inconsistency may explain a large portion of the discrepancy often found between NMR- and fluorescence-derived τ_m values for proteins. The near identity of observed T_2 and $T_{1\rho}$ values suggests that contributions from slow motions are not the origin of the apparent inconsistency with obtained T_1 and NOE data. Various considerations suggest that the origin of this apparent discrepancy may reside in a contribution to the spectral density at zero frequency that is not represented by the simple model-free formalism in addition to the usual experimental difficulties associated with the measurement of these relaxation parameters. Finally, an axially symmetric diffusion tensor for ubiquitin is obtained using exclusively T_1 and NOE data. A recommendation is reached on the types and combinations of relaxation data that can be used to reliably determine τ_m values. It is also noted that the reliable determination of τ_m values from ^{15}N T_1 and NOE relaxation parameters will become increasingly difficult as τ_m increases.

Abbreviations: NOE, nuclear Overhauser effect; $\Delta\sigma$, chemical shift anisotropy; τ_m, global rotational correlation time; S^2, square of the generalized order parameter; τ_e, internal correlation time; T_1^{51} (or T_2^{51}, NOE^{51}), T_1 (or T_2, NOE) measured at 51 MHz ^{15}N frequency.

Introduction

^{15}N spin relaxation is a useful probe of protein dynamics in solution (Peng and Wagner, 1994; Palmer et al., 1996). Typically, dynamics are characterized from measurements of T_1, T_2, and $\{^1$H$\}$-^{15}N NOE, the precise combination of observables employed often arising out of convenience. Relaxation of longitudinal and transverse magnetization is mediated by fluctuations in N-H bond vector orientations provided by overall rotational tumbling, as well as internal dynamic motions. Because the relaxation rates encoun-

*To whom correspondence should be addressed.
Supplementary material: Tables containing ^{15}N T_1, T_2, and NOE relaxation parameters and best-fit S^2, τ_e, and $\Delta\sigma$ values from T_1 and NOE data have been deposited into the BioMagResBank (Accession Number 4245).

tered in structured proteins are most often dominated by overall tumbling, the determination of the overall correlation time (τ_m) is crucial for any subsequent dynamics analysis if a separation between tumbling and internal motion is desired. This separation is normally accomplished by employing the 'model-free' formalism (Lipari and Szabo, 1982a,b). In this treatment, τ_m is an isotropic rotational correlation time, and S^2 and τ_e are model-independent parameters that describe the internal motion(s). The square of the generalized order parameter (S^2) describes the degree of spatial restriction of the bond vector in the molecular frame, and τ_e is the effective correlation time for the internal motion. This formalism has the flexibility to incorporate anisotropic tumbling, although isotropic tumbling has been used for most studies to date. In any case, for globular proteins, accounting for the slight anisotropies has a negligible effect on the extracted dynamics parameters (Tjandra et al., 1995).

Here we are concerned with the methods by which a reliable description of the slow motional component, often associated with global tumbling, is determined. Historically, three approaches have emerged. The most frequently used method for determining τ_m is to employ ^{15}N T_1/T_2 ratios – or an average of such ratios – of amides involved in secondary structure to estimate an isotropic τ_m (Kay et al., 1989). Because a simplified or reduced form of the spectral density is used [$J(\omega) = S^2\tau_m/(1+\omega^2\tau_m^2)$], this method requires that internal motions be sufficiently fast so as not to affect the T_1/T_2 ratio. Global correlation times have also been obtained via extensive optimization during global model-free fits (Dellwo and Wand, 1989). This involves fitting S^2 and τ_e for each site for a series or 'grid' of global τ_m values and identifying the τ_m which minimizes a global error function. Here, a minimum of $2n + 1$ determined relaxation parameters for n sites are required. A similar method is to fit τ_m locally for each site, which requires additional relaxation parameters to be determined. In this case, the obtained parameters for a given amide are independent of all other residues, and the set of τ_m values contains information about tumbling anisotropy (Barbato et al., 1992; Schurr et al., 1994). These last two methods differ from the T_1/T_2 method in that they explicitly account for internal motions, which does not usually alter the obtained τ_m in the case of ^{15}N relaxation. However, not accounting for internal motions would appear to be a poor approximation when ^{13}C relaxation is used to determine τ_m, as is discussed below. More recently, Wagner and co-workers have described a method using the reduced spectral density mapping technique (Lefevre et al., 1996). This method appears to make similar assumptions to those made by Lipari and Szabo, and the resultant τ_m values are comparable.

Once obtained, τ_m can be held fixed, and S^2 and τ_e can be obtained in a straightforward manner. However, because S^2 and τ_e are strongly dependent on τ_m, an inaccurate determination of τ_m can result in erroneously fitted model-free parameters, as previously pointed out (Korzhnev et al., 1997). Another consideration is the possibility that the final τ_m obtained may be sensitive to the types of relaxation data included in the analysis. T_1, T_2, and NOE are routinely collected, but in some cases only T_1 and NOE have been used. With this in mind, it is interesting to note that fluorescence-derived τ_m values are often found to be shorter than NMR-derived τ_m values, as in the cases of a zinc-finger peptide (Palmer et al., 1993), thioredoxin (Kemple et al., 1994), and lysozyme (Dubin et al., 1971; Buck et al., 1995). Because of these discrepancies, the most reliable methods for determining τ_m should be sought.

Materials and methods

Sample preparation

Uniformly ^{15}N-labeled human ubiquitin samples were prepared as previously described (Wand et al., 1996). Lyophilized protein was dissolved in 650 μl of buffer containing 90% H_2O/10% D_2O, 50 mM acetate-d_3, pH 5.0, and 0.02% NaN_3. The final protein concentration was 4 mM.

NMR spectroscopy

Relaxation measurements were made on Varian Inova spectrometers at 11.7, 14.1, and 17.6 Tesla. All Varian spectrometers were equipped with standard Varian ^{1}H/^{15}N/^{13}C probeheads with z-axis pulsed field gradients. Additional data was collected on a wide bore Bruker DMX-400 (9.4 T) equipped with a ^{1}H/^{15}N/^{13}C/^{31}P probehead with z-axis gradients (at the University of Wisconsin at Madison). ^{15}N T_1 experiments were carried out on ubiquitin at 40.55, 50.66, 60.79, and 76.08 MHz field strengths, hereafter referred to as T_1^{41}, T_1^{51}, T_1^{61}, and T_1^{76}, respectively. {^{1}H}-^{15}N NOE experiments were also carried out at 51, 61, and 76 MHz. ^{15}N T_2 measurements were made at 51 MHz. Additional ^{15}N T_2 measurements were made at 61 MHz to compare with $T_{1\rho}$ measurements made at this field strength. All measurements were

calibrated to a temperature of 25 °C using a 100% methanol standard (Raiford et al., 1979).

The two-dimensional heteronuclear sampling technique was used for the measurement of ^{15}N T_1 (Nirmala and Wagner, 1988) and T_2 (Palmer et al., 1992), and the {^{1}H}-^{15}N NOE was measured from experiments with and without ^{1}H saturation (Kay et al., 1989). For the T_1 experiment, a difference T_1 time course was utilized to ensure that the observed signals decayed to zero (Sklenar et al., 1987). During the longitudinal relaxation period, 120° ^{1}H pulses were placed every 5 ms to remove effects from cross-relaxation and dipolar/CSA cross-correlation. For the T_2 experiment, ^{15}N 180° pulses in the CPMG train were spaced by 900 μs, and ^{1}H 180° pulses were centered in the CPMG block in order to remove effects from dipolar/CSA cross-correlation (Goldman, 1984; Palmer et al., 1992). Recycle delays in the T_1 and T_2 experiments were typically ∼1.1 s. All pulse sequences employed sensitivity-enhanced gradient selection of ^{15}N coherence (Farrow et al., 1994). Minimal perturbation of the water resonance was used in the NOE experiment but not in T_1 or T_2 experiments. The pulse sequence for measurement of $T_{1\rho}$ was essentially that for measuring T_2, in which the CPMG pulse train was replaced by a ^{15}N spin-lock during which high power ^{1}H 180° pulses were spaced by 5 ms.

T_1 relaxation delay times at the 4 field strengths were as follows. Duplicate measurements are indicated with asterisks. At 9.4 T: 35.0*, 59.9, 89.8, 129.7*, 179.6, 229.5, 294.4, 359.3, 434.1*, 514.0, 603.8, 703.6 ms. At 11.7 T: 46.4*, 81.6, 126.8*, 182.1, 252.4*, 327.8, 413.2, 513.7, 619.2*, 734.7, 865.4, 1006.0 ms. At 14.1 T MHz: 91.6*, 146.8, 212.1, 292.5*, 377.9, 483.3, 593.8*, 719.4, 855.0, 1005.6 ms. At 17.6 T: 76.5*, 106.6, 146.7*, 191.9, 242.0, 302.2*, 362.4, 432.7, 507.9, 588.2*, 678.5, 768.8, 869.2*, 974.6, 1084.9, 1205.3 ms. For T_2 relaxation measurements at 11.7 T, CPMG pulse trains of 8.0*, 16.0, 23.9, 31.9*, 47.9, 55.9, 63.8, 71.8, 87.8* ms in length were used and employed a 5.1 kHz ^{15}N RF field. For T_2 relaxation at 14.1 T, CPMG pulse trains of 7.8, 15.7, 23.5, 39.2, 62.7, 78.4, and 109.8 ms in length were used and employed a 6.25 kHz ^{15}N RF field. Longer T_2 relaxation times were not used because they resulted in sample heating, which results in overestimated T_2 values. $T_{1\rho}$ relaxation delays (at 14.1 T) were set to 10.0*, 20.1, 30.1*, 40.1, 55.2, 70.2*, 90.3, 110.4, 135.4 ms, and a spin-lock power of 3.5 kHz was used. Sample heating in the $T_{1\rho}$ experiment was minimized by using a 3 s recycle delay. In the {^{1}H}-^{15}N NOE experiments, a steady state was reached after at least 3 s of 120° ^{1}H saturation pulses spaced every 5 ms, and a total recycle delay time of 5 s was used to allow for longitudinal magnetization to reach equilibrium. Spectra with and without the NOE were collected in an interleaved manner. For T_1 and T_2 data sets, duplicate points were acquired to aid in error estimation of peak intensities. For all experiments, the ^{15}N carrier was placed in the center of the ubiquitin HSQC spectrum, at 116 ppm. Typically, the ^{15}N spectral width was set to 34 ppm, and 100 complex t_1 points were collected. For the T_1 and T_2 experiments, 8 scans per FID were recorded, and 16 scans per FID were recorded for the NOE experiment. For T_1 experiments at 41 MHz, 24 scans per FID were recorded.

Data analysis

All data sets were processed into 512 × 1024 matrices using Felix 95.0 (Molecular Simulations Inc., San Diego, CA). The resonance assignments for ubiquitin have been previously reported by us (Di Stefano and Wand, 1987; Schneider et al., 1992; Wand et al., 1996). Cross peak intensities were used to quantitate ^{15}N magnetization. The Levenberg-Marquardt algorithm (Press et al., 1992) was used for two-parameter curve-fits for T_1, T_2, and $T_{1\rho}$ decays. Fitted $T_{1\rho}$ values were subsequently corrected for resonance offset effects (Peng and Wagner, 1994). On the whole, χ^2 residuals were lower than the number of data points in a given decay, signaling 'good fits'. All relaxation parameters are reported in the supplementary material. Standard errors in the relaxation rate constants were taken from the covariance matrix, and re-acquisition of T_1 data sets confirmed this procedure. Standard errors in T_1 values were 1% for 51, 61, and 76 MHz data sets, and 0.7% for the 41 MHz data set. The T_2 values had errors of ∼2% at 51 MHz and 61 MHz. $T_{1\rho}$ values at 61 MHz had errors of ∼1.2%. {^{1}H}-^{15}N NOEs were calculated from peak intensity ratios, I^{NOE}/I^{ref}, in the NOE (^{1}H saturation) and reference (no ^{1}H saturation) experiments. Intensity uncertainties were estimated from the rms noise level in the baseplane. To be conservative, this value was doubled and then propagated to yield standard errors of ∼2% for 51 and 61 MHz data sets, and ∼1% for the 76 MHz data set. Residue amides 19, 21, 24, 28, 31, 37, 38, 53, 61, 69, 71, 72, and 73 were excluded from the analysis due to spectral overlap or because they gave rise to very weak cross peaks. The expressions governing ^{15}N spin relaxation are well known (Abragam, 1961) and will

not be reproduced here. Axial symmetry for the CSA tensor ($\Delta\sigma = \sigma_{\parallel} - \sigma_{\perp}$) is assumed, with some experimental justification, although expressions also exist for asymmetric chemical shift tensors (Kemple et al., 1994; Kowalewski and Werbelow, 1997). The model-free spectral density, $J(\omega)$, for a molecule tumbling isotropically is given by (Lipari and Szabo, 1982a)

$$J(\omega) = \frac{2}{5}\left[\frac{S^2\tau_m}{1+\omega^2\tau_m} + \frac{(1-S^2)\tau}{1+\omega^2\tau^2}\right] \quad (1)$$

in which $\tau^{-1} = \tau_m^{-1} + \tau_e^{-1}$, τ_e is the internal correlation time constant, τ_m is the overall correlation time, and S^2 is the square of the so-called generalized order parameter.

Dynamics parameters (and in some cases $\Delta\sigma$) were fitted locally for each residue using either a grid search or a Powell minimization (Press et al., 1992) of the error function:

$$\chi^2 = \sum_j^M \left(\frac{obs_j - calc_j}{\lambda_j^{obs}}\right) \quad (2)$$

where M is the number of relaxation measurements for a given spin, obs_j is the j^{th} measured relaxation parameter, $calc_j$ is the j^{th} calculated relaxation parameter, and λ_j^{obs} is the estimated uncertainty in obs_j. ^{15}N $\Delta\sigma$ was fixed at -170 ppm if it was not an adjustable parameter, and the N-H bond distance, r_{NH}, was taken to be 1.02 Å. Because the Powell procedure does not find global minima, an initial grid search of the relevant parameter space was performed prior to Powell. Parameter errors were estimated from 150–500 Monte Carlo simulations.

It should be noted that τ_m reported here for 4 mM ubiquitin is expected to be longer than that reported previously for 1.5 mM ubiquitin (Tjandra et al., 1995) due to the slight temperature difference (25 °C vs. 27 °C) and difference in solution viscosity due to higher protein concentration (Tanford, 1961; Cantor and Schimmel, 1980). This concentration effect is significant even in the absence of aggregation; using an intrinsic viscosity of 3.3 $cm^3\ g^{-1}$ for ubiquitin, the viscosity is predicted to increase 8% between 1.5 and 4 mm at a given temperature. At 25 °C, T_1^{51} values increased ~6% going from 1.0 mM to 4 mM ubiquitin, consistent with a 15–20% increase in τ_m (data not shown). Similarly, the average T_1^{61} values for 4 mM ubiquitin here are ~5% longer than the average T_1^{61} values for 1.5 mM ubiquitin at 27 °C. It is possible that non-specific aggregation increases τ_m by up to 5% at 4 mM. However, because no evidence for slow chemical exchange contributions to T_2 was observed (see below), small degrees of non-specific aggregation should not introduce bias into τ_m values derived with or without T_2. In summary, accounting for temperature and protein concentration reconciles the different T_1, T_2, and τ_m values observed for 1.5 and 4 mM ubiquitin.

Rotational diffusion tensors were fitted using in-house written software or software made available by Dr. Art Palmer (Columbia University). The local D_i approach was used (Brüschweiler et al., 1995; Lee et al., 1997). Standard errors for tensor components were obtained from Monte Carlo simulations.

Results and discussion

The determination of τ_m describing overall rotation for ubiquitin was carried out using the local site treatment of Schurr and coworkers (Schurr et al., 1994), as this has been shown to be more informative than the globally linked approach (Dellwo and Wand, 1989). In the local site approach, S^2, τ_e, and τ_m are each fitted as local dynamics parameters using the error function defined in Equation 2. Isotropic, global τ_m values for the protein were obtained from an uncertainty weighted average (Taylor, 1982) of these local τ_m values from rigid regions of ubiquitin. This method for determining the global τ_m is essentially equivalent to the globally linked approach, only in principle it has the advantage of being less sensitive to poor model-free fits arising from individual spins.

Residue amides 8–12, 48, 49, 62, and 74–76 were excluded from the analysis, based on deviations from average NOE values. If T_2 was used in the analysis, residues 18, 23, 25, and 36 were also excluded, since these residues were shown to exhibit effects from conformational exchange (Tjandra et al., 1995). Results of τ_m determinations from the model-free fits are given in Table 1. For all fits, the goodness of fit was assessed using a reduced χ^2 statistic, χ^2_{M-n}, defined as χ^2 divided by the degrees of freedom (i.e. number of data measurements minus number of model parameters).

Initially, we employed relaxation data obtained at 11 T and 14 T (T_2^{51}, $T_1^{51,61}$ and $NOE^{51,61}$) and τ_m was determined to be 4.6 ns and the average χ^2_{M-n} was 3.61. Curiously, this relatively poor goodness-of-fit was considerably improved when only $T_1^{51,61}$ and $NOE^{51,61}$ data were used and a τ_m of 4.0 ns and average χ^2_{M-n} (per residue) of 2.64 were obtained. This corresponds to 1–2% agreement between experimen-

Table 1. Summary of three- and four-parameter fits to ubiquitin ^{15}N relaxation data at 25 °C[a]

Data combination[b]	Degrees of freedom (M–n)	$<\chi^2_{M-n}>$[c]	τ_m (ns)[d]	^{15}N $\Delta\sigma$ (ppm)[e]
A {T_1,NOE}	1	2.64	4.00	–
B {T_1,NOE}	2	2.34	4.20	–
C {T_1,NOE}	4 (3)	2.60 (2.50)	4.15 (4.03)	(−173)
D {T_1,T_2,NOE}	2	3.61	4.58	–
E {T_1,T_2,NOE}	4 (3)	4.35 (3.03)	4.49 (4.62)	(−190)
F {T_1,T_2,NOE}	5 (4)	4.93 (2.76)	4.42 (4.61)	(−189)

[a] Three-parameter fits had S^2, τ_e, and τ_m as local adjustable parameters. Four-parameter fits had S^2, τ_e, τ_m, and ^{15}N CSA ($\Delta\sigma$) as local adjustable parameters. Results from four-parameter fits are given in parentheses. $\Delta\sigma$ was set to −170 ppm for the three-parameter fits.

[b] (A) $T_1^{51,61}$, NOE^{51,61}; (B) $T_1^{41,51,61}$, NOE^{51,61}; (C) $T_1^{41,51,61,76}$, NOE^{51,61,76}; (D) $T_1^{51,61}$, T_2^{51}, NOE^{51,61}; (E) $T_1^{51,61,76}$, T_2^{51}, NOE^{51,61,76}; (F) $T_1^{41,51,61,76}$, T_2^{51}, NOE^{51,61,76}.

[c] χ^2_{M-n} is the reduced chi-squared statistic (see text). The average is taken over all residues.

[d] τ_m was computed as an uncertainty weighted average over all residues (Taylor, 1982). Statistical uncertainties in τ_m were 0.04, 0.02, 0.01 (0.03), 0.01, 0.01 (0.01), and 0.01 (0.01) ns for data combinations A–F, respectively.

[e] $\Delta\sigma$ was computed as an uncertainty weighted average over all residues. $\Delta\sigma$ was only fitted when T_1^{76} and NOE^{76} data were included in the analysis.

tal and back-calculated relaxation parameters for most residues. If T_1/T_2 ratios were used, τ_m was also determined to be 4.6 ns. The fact that inclusion of T_2 data significantly raised χ^2_{M-n} (per residue) suggests that they are somewhat inconsistent with the T_1 and NOE data, an observation previously made by Prendergast and co-workers (Kemple et al., 1994). To explore the origin of this apparent inconsistency, we have taken advantage of the unusually large set of relaxation parameters determined which allows the combinatorial dependence of the obtained model-free parameters on the observed relaxation parameters to be examined.

The apparent inconsistency of T_2

The measurement of ^{15}N longitudinal magnetization is well documented (Peng and Wagner, 1994, and references therein) and arguably the simplest relaxation experiment with the highest accuracy. In the following, T_1 has therefore been included in all analyses, assuming that the measured T_1 values at all fields contain no systematic errors. The importance of T_2 and NOE measurements for extracting dynamics parameters was tested by analyzing $T_1^{41,51,61}$ data in addition to either T_2^{51} or NOE^{51}. When only T_1 and T_2 were used, the obtained τ_m values were consistently over 5 ns and τ_e values uniformly approached 500 ps. In contrast, when only T_1 and NOE were used, reasonable parameters were obtained ($\tau_m \sim 4$ ns, $\tau_e <$ 100 ps). If the τ_e values were truly on the order of 500 ps as suggested by the T_1, T_2 combination, NOE values should fall in the range of 0.4–0.5, suggesting that the measured NOE values are in error by 30%, which seems unlikely. This argues for inclusion of at least one set of NOE data, as previously pointed out (Dellwo and Wand, 1991), whereas T_2 may or may not be expendable. Given this, it is not useful to compare {T_1, *NOE*} combinations against {T_1, T_2} combinations and we concentrate further on the comparison of {T_1, *NOE*} and {T_1, T_2, *NOE*} combinations.

As T_1^{76} and NOE^{76} measurements were also made, fits of S^2, τ_e, and τ_m were repeated using $T_1^{41,51,61,76}$, NOE^{51,61,76}, and with or without T_2^{51}. Fits not employing T_2 yielded a τ_m of 4.15 ns and χ^2_{M-n} of 2.60, whereas when T_2 was included a τ_m of 4.42 ns and χ^2_{M-n} of 4.93 were obtained. Of concern at very high field strengths is the contribution to relaxation due to CSA, which increases as the square of the field. If there is any inconsistency between the true and assumed (−170 ppm) CSA values, the fits will probably compensate for the inconsistency by adjustment of other fitted parameters (for example, see Figure 5 of Schneider et al., 1992). Experimental measurements

of ^{15}N amide chemical shift tensors have been made using various methods, and an average value for the CSA breadth ($\Delta\sigma$) of -170 ppm has emerged (Oas et al., 1987; Hiyama et al., 1988; Tjandra et al., 1996b; Ottiger et al., 1997). This average value, with an associated variability of ± 15 ppm for different residues in ubiquitin, has also been obtained in a quite different manner (Tjandra et al., 1996a). With this degree of uncertainty for individual $\Delta\sigma$ values, T_1^{76} values could correspondingly be misinterpreted by as much as $\sim$5%. On the other hand, if the field-dependent $\Delta\sigma$ contribution to relaxation can be realized from the data along with the model-free parameters, it should be possible to use the known average of $\Delta\sigma$ to evaluate the degree of self-consistency associated with different τ_m values obtained from ^{15}N relaxation.

Using data at all fields, an attempt was made to recover the individual ^{15}N $\Delta\sigma$ values for each residue, assuming axial symmetry of the CSA tensor, in addition to local S^2, τ_e, and τ_m parameters. The results are summarized in Table 1 (4-parameter fits are in parentheses). The significant observation from these fits was that different values for τ_m and $\Delta\sigma$ were obtained depending on whether T_2 was included in the data set. When T_2 was employed, uncertainty weighted averages of τ_m and $\Delta\sigma$ were 4.62 ns and -190 ppm, respectively, whereas in the case using only T_1 and NOE data, the obtained averages for τ_m and $\Delta\sigma$ were 4.03 ns and -173 ppm. When T_2 was included, larger $\Delta\sigma$ and τ_m values clearly served to reduce T_2^{calc} (so that they were more consistent with T_1 and NOE) while having a counteracting effect on 76 MHz T_1^{calc} values. This explains the substantial reduction in χ^2_{M-n} upon treating CSA as the fourth adjustable parameter. When τ_m was fixed at the overall consensus value of 4.1 ns consistent with T_1 and NOE data (Table 1), T_1 and NOE data yielded individually fitted $\Delta\sigma$ values of -169 $\pm$10–15 ppm, suggesting that this value of τ_m is indeed physically reasonable. Results from these 3-parameter fits are given in the supplementary material. The fitted values of $\Delta\sigma$ increased when τ_m was increased (data not shown). Thus one is led to conclude that T_1 and NOE data can reliably provide estimates of global and local motion. In contrast, it appears that the T_2 data, although measured very carefully and numerous times, influences the fits to yield physically unreasonable fitted parameters ($\Delta\sigma = -190$ ppm).

Origin of the apparent inconsistency of T_2

Simulations were carried out in order to test if T_2 could influence the fits in this way. $T_1^{51,61,76}$, T_2^{51}, and NOE^{51,61,76} data were calculated at various field strengths for τ_m of 4.0 ns, S^2 of 0.8, τ_e of 20 ps, and a CSA breadth of -170 ppm. The simulated T_2^{51} value was artificially lowered or raised in independent data sets, resulting in a series of data sets in which only T_2^{51} was varied. Random errors of 1% were assigned to each observable except T_2^{51}, which was assigned 2.5% error (matching the error magnitudes in the real data sets). Each data set was then analyzed using the 4-parameter fitting procedure (S^2, τ_e, τ_m, $\Delta\sigma$). The results are summarized in Table 2. The experimental scenario, i.e. increased τ_m and $\Delta\sigma$ obtained from {T_1, T_2, NOE} data relative to {T_1, NOE} data, is reproduced when T_2 is artificially reduced by 10–15% in the simulations. This suggests that the experimental T_2 values on ubiquitin are 10–15% shorter than an ideal T_2 consistent with the Lipari-Szabo description of protein dynamics. Correspondingly, τ_m may be overestimated by 10–15% if T_2 data is used to determine τ_m. It is alternatively conceivable that the NOE measurement could be a source of contamination. This was tested similarly, and the only way in which the experimental scenario could be reproduced is if the NOE is systematically low, or overdeveloped. It is difficult to come up with a plausible reason for an overdeveloped, as opposed to an underdeveloped, NOE.

There are many possible mechanisms that can lead to an underestimation of heteronuclear spin-spin relaxation in the laboratory frame. These include the presence of μs–ms timescale motions (Deverell et al., 1970), contribution from antiphase magnetization (Peng and Wagner, 1994), scalar relaxation (Abragam, 1961), off-resonance effects during the CPMG pulse train (Ross et al., 1997), and simple technical issues such as ^{15}N pulse imperfections. In principle, measuring $T_{1\rho}$ instead of T_2 should alleviate a number of problems associated with the CPMG pulse train (Peng et al., 1991): the contribution from heteronuclear antiphase magnetization should be removed; motions on a timescale slower than the spin-lock field strength (i.e. milliseconds) will cease to contribute to transverse relaxation; off-resonance effects should be correctable; and effects from pulse imperfections will not accumulate as in CPMG (Simbrunner and Stollberger, 1995). Surprisingly, $T_{1\rho}^{61}$ values obtained here for ubiquitin were on the average 2–3% lower than

Table 2. Simulation of fitting four parameters with introduction of error in T_2[a]

T_2 error	τ_m (ns)	S^2	τ_e (ps)	^{15}N $\Delta\sigma$ (ppm)
−20%	4.84	0.803	36.3	−195.4
−15%	4.59	0.800	31.9	−188.4
−10%	4.37	0.799	27.8	−181.8
−5%	4.18	0.799	23.8	−175.7
0%	4.00	0.800	20.0	−170.1
5%	3.85	0.801	16.4	−165.2
10%	3.72	0.802	13.0	−161.0
15%	3.60	0.803	9.9	−157.6
20%	3.51	0.803	6.9	−154.6

[a] Relaxation data was simulated for a single ^{15}N spin with $\tau_m = 4.0$ ns, $S^2 = 0.8$, $\tau_e = 20$ ps, and $\Delta\sigma = -170$ ppm: $T_1^{51,61,76}$, T_2^{51}, and NOE^{51,61,76}. T_1 and NOE data were given 1% uncertainties, and T_2 data was given 2.5% uncertainty. These uncertainties were used only for weighting purposes in Equation 2. T_2 values were changed by the indicated amount, and these data sets were least-squares fitted to the four parameters.

corresponding T_2^{61} values (Supplementary material), although identical values within experimental uncertainty were obtained for amides which resonate within ∼100 Hz of the nitrogen carrier frequency.

There are three possible interpretations of the observed discrepancy between the experimental T_1/NOE and transverse relaxation data. The first is simply that both measured T_2 and $T_{1\rho}$ values are shorter than expected from the theory of transverse relaxation, perhaps suggesting the presence of additional unaccounted for relaxation mechanisms. RF inhomogeneity in the ^{15}N spin-lock can lead to underestimatation of $T_{1\rho}$. As a second interpretation, ubiquitin may experience pervasive microsecond timescale motions which would shorten both T_2 and $T_{1\rho}$ via chemical exchange processes (Akke et al., 1998). This appears to be unlikely based on $R_{1\rho}$–R_1 experiments (Akke and Palmer, 1996) carried out on ubiquitin, which do not detect any exchange events on timescales down to ∼25 μs (data not shown). The average ratio of T_2^{51}/T_2^{61}, which was determined to be 1.04, is also consistent with a lack of chemical exchange contributions to T_2 and $T_{1\rho}$ measurements, assuming a CSA value of −170 ppm. The third interpretation is that T_2 and $T_{1\rho}$ may be accurately reporting on additional dynamics which are manifest at $J(0)$ but not at the higher sampling frequencies. This would imply that the model-free spectral density is quantitatively inappropriate in this case. Although this possibility is intriguing from the perspective of the internal dynamics, the point to be stressed is that both T_2 and $T_{1\rho}$ parameters obtained here for ubiquitin appear unreliable for the accurate determination of model-free parameters, and in particular, τ_m.

An obvious physical origin for deviation from a simple Lorentzian spectral density can be found in emerging theoretical views of the dynamics of complex polymers such as proteins. For some time it has been appreciated that slower (i.e., microsecond) nonequilibrium protein fluctuations usually assume complex time dependencies that are often conveniently described by 'stretched' exponentials (Frauenfelder and Wolynes, 1985; Frauenfelder et al., 1991). Recent theoretical treatments of the gated diffusion problem have illuminated the origin of this class of polymer motion (Zhou and Zwanzig, 1991; Wang and Wolynes, 1993). In several respects, the presence of this type of motion in the nanosecond time regime would violate the assumptions of the Lipari and Szabo treatment and could lead to significant deviation from the underlying Pade approximation (Lipari and Szabo, 1982a,b). Specifically, the spectral density arising from such an autocorrelation function would have significantly more intensity at zero frequency than the corresponding Lorentzian spectral density.

Determining τ_m without T_2 data

From these results, it appears that the T_2 and $T_{1\rho}$ values that we have obtained for ubiquitin are systematically lower than those predicted by measured T_1 and NOE parameters in the context of a model-free analysis. One can imagine that this reflects a deviation of the underlying spectral density from the simple Lorentzian form assumed by the model-free treatment and/or experimental difficulties in obtaining accurate spin-spin relaxation times. Such inaccuracies can skew the obtained dynamics parameters or any other quantities extracted from the relaxation data, the specific parameters skewed (and the direction) being a somewhat complicated function of the set of fitted parameters and the types of relaxation data included in the analysis. Should the measurement of T_2 ($T_{1\rho}$) be generally susceptible to these complications, the safest route to an accurate characterization of fast (sub-τ_m) dynamics of proteins may involve analysis of T_1 and NOE data only. This would emphasize the region of the spectral density that is anticipated to most closely satisfy the model-free form. Unfortunately, as protein size increases the robustness of T_1 and NOE data to determine τ_m diminishes. We illustrate this in Figure 1, which summarizes simulations in which

Gaussian noise was introduced into perfect ^{15}N relaxation data and subsequently fitted to model-free parameters (S^2, τ_e, τ_m). It is seen that as the true τ_m increases, it becomes increasingly difficult to reliably fit τ_m without good T_2 data. The essence of the problem lies in defining a Lorentzian function (corresponding to the first term in Equation 1) based on frequencies which fall increasingly further out on the tail of $J(\omega)$ as τ_m passes into the slow correlation time limit. Because S^2 and τ_e must also be fitted simultaneously, small uncertainties in T_1 values for $\omega_v\tau_m >> 1$ project into large uncertainties in $J(\omega)$ at low frequencies. Therefore, even though T_1 is quite sensitive to τ_m, fitting out reliable values of τ_m can be difficult, as proven by the simulations in Figure 1. Accordingly, the T_1 data become decreasingly sensitive to overall rotation and increasingly sensitive to fast internal motion as $\omega\tau_m$ increases. In these simulations it is evident that if only T_1 and NOE data is used, lower field strengths will be required to fit data for larger proteins. As long as $\omega\tau_m \leq 1$, T_2 should not be necessary for the reliable determination of τ_m. It is important to note that regardless of the precise nature of the spectral density describing internal motion, the combined use of only T_1 and NOE data provides an adequate means to confidently extract accurate isotropic τ_m values using the model-free approach.

For typical ^{15}N relaxation data sets (T_1 and NOE at 51 and 61 MHz, with T_1 uncertainties at 1–2%) across ~75 sites, simulations suggest that it should be possible to reliably determine an isotropic, global τ_m of up to about 7 ns from an uncertainty weighted average of locally fitted τ_m values. In certain cases, it may be necessary to use transverse relaxation parameters and accept the potential for an inflationary effect on the obtained molecular reorientation time. Other longitudinal relaxation experiments which probe low frequency regions of the spectral density, such as the {$^{13}C_\alpha$}-^{13}CO NOE experiment (Cordier et al., 1996; Zeng et al., 1996), may help to interpret the apparent discrepancies reported here and also to extend the range of reliably determined τ_m values.

Effect on obtained model-free parameters

A consequence of shorter τ_m resulting from exclusion of T_2 for typical ^{15}N or ^{13}C relaxation data ($\omega_N\tau_m > 1$) is that S^2 will be fitted to lower values (Schurr et al., 1994). As shown in Figure 2a, when {T_1, T_2, NOE} data was used, the fitted τ_m was 4.6 ns and the order parameters were approximately 5% larger than those fitted from {T_1, NOE} data, from which τ_m was de-

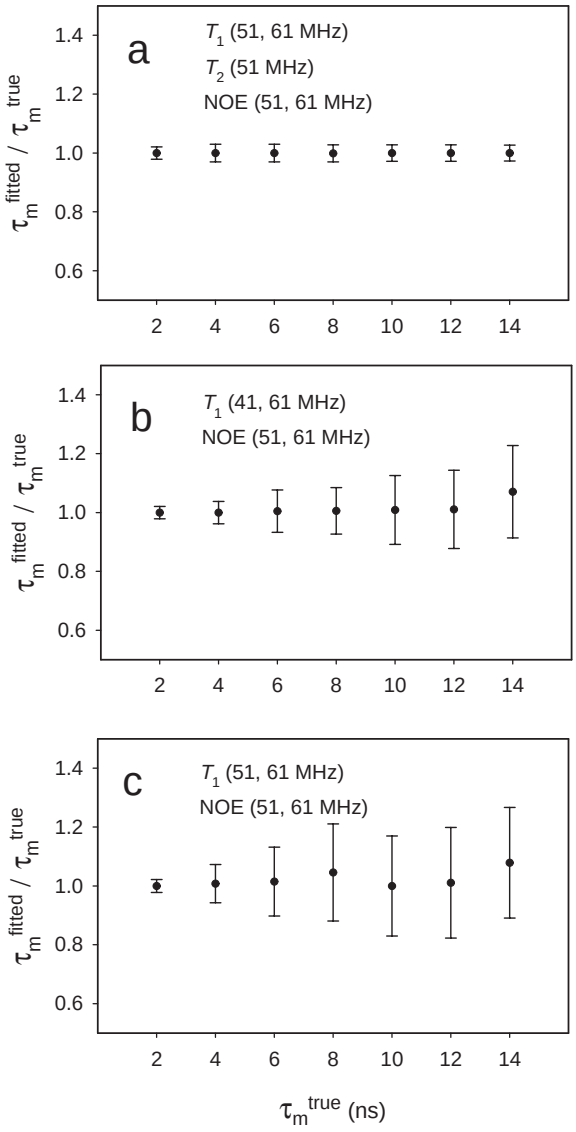

Figure 1. Least-square fits of τ_m to various combinations of simulated data. Relaxation data at 41, 51, and 61 MHz were simulated for a single ^{15}N spin with $S^2 = 0.8$, $\tau_e = 20$ ps, CSA $= -165$ ppm, and the indicated values of τ_m (2–14 ns). T_1 and NOE data were given 1% error. T_2 data was given 5% error. A three-parameter fit (S^2, τ_e, τ_m) was performed in all cases using data combinations (a) $T_1^{51,61}$, T_2^{51}, NOE^{51,61}; (b) $T_1^{41,61}$, NOE^{51,61} and (c) $T_1^{51,61}$, NOE^{51,61}. Error bars correspond to standard deviations obtained from Monte Carlo simulations of the fits.

termined to be 4.1 ns. Employing larger fixed values of CSA also has the effect of decreasing the fitted order parameters. Therefore, using the recommendations below for fitting model-free parameters, we expect that order parameters will *decrease* relative to those obtained by the standard method (i.e. obtaining τ_m from T_1/T_2 ratios and using CSA $= -160$ ppm). A similar but more dramatic effect on τ_e (by percentage) is observed with varying τ_m values. However, because uncertainties in τ_e are usually relatively large, the effect does not appear to be very significant.

In Figure 2b, {T_1, NOE} and {T_1, T_2, NOE} data combinations were used for local 4-parameter fits (S^2, τ_e, τ_m, $\Delta\sigma$), and the agreement between S^2 values was much higher. Apparently, the effects of T_2 have been primarily absorbed in the τ_m and $\Delta\sigma$ parameters and not in S^2 (also see Table 2). However, if $\Delta\sigma$ is fixed, the effects of T_2 are absorbed in τ_m and S^2. The excellent correlation between S^2 determined from the two data combinations suggests that the S^2 values determined from the 4-parameter fits are the most accurate.

Anisotropic tumbling

Ubiquitin has been shown to tumble with a small degree of anisotropy which is axially symmetric (Tjandra et al., 1995), perhaps complicating the present analysis since an isotropic model has been used. However, because τ_m was fitted locally for all cases, anisotropy should not pose any difficulties. Instead, the local τ_m will actually be $\tau_{m,eff}$, given by

$$\frac{1}{\tau_{m,eff}} = 6D_{eff} \tag{3}$$

$$D_{eff} = \frac{1}{3}\left(D_{xx} + D_{yy} + D_{zz}\right) \tag{4}$$

in which D_{ii} are the diagonal components of the rotational diffusion tensor. To a good approximation (Schurr et al., 1994; Brüschweiler et al., 1995; Lee et al., 1997), a spin behaves like an isotropic tumbler with a rotational correlation time of $\tau_{m,eff}$, and the fitting of parameters (S^2, τ_e, or $\Delta\sigma$) should be insignificantly different than for a truly isotropically tumbling protein.

A potential complication of second order is that rotational anisotropy will affect dipolar and CSA relaxation mechanism contributions differently if the orientation of the N-H bond vector and CSA principal axis are not collinear. In this case, when the 4-parameter fits (S^2, τ_e, τ_m, $\Delta\sigma$) are performed, there is a danger of τ_m absorbing CSA effects and vice versa. This could also occur even when fitting S^2, τ_e, and τ_m locally if high-field data is used. However, because (1) the rotational anisotropy of ubiquitin is small; (2) the angle between the N-H bond vector and the CSA principal axis is small, ~13–16° (Ottiger et al., 1997); and (3) dipolar and CSA relaxation contributions have distinct field dependencies, this is not likely to be a problem here. In addition, the effect on *average* τ_m and $\Delta\sigma$ values would be even smaller since the effects will tend to cancel out over a number of residues and their respective N-H and CSA orientations.

It is nevertheless interesting to note that the present results may have implications for determining anisotropic diffusion tensors. To the best of our knowledge, for all cases in which anisotropic diffusion tensors have been determined for proteins, T_2s have been used extensively. If determined T_2 values do indeed contain systematic and random errors from the above-mentioned effects or if they reflect more complex dynamics, caution should be exercised in using these measurements to determine rotational diffusion tensors. Nevertheless, for proteins with significant anisotropy, only the magnitude of the obtained diffusion tensor is likely to be affected if bias in T_2 is uniformly distributed over the protein, such as may be the case in the ubiquitin data (−10 to −15% apparent underestimation).

In principle, it is possible to fit an anisotropic diffusion tensor using only T_1 and NOE data. Results from the local D_i approach (Brüschweiler et al., 1995; Lee et al., 1997) are given in Table 3. Local D_i ($= 1/6\tau_m$) were obtained from a $T_1^{41,51,61}$ and $NOE^{51,61}$ data set or from a data set comprised of $T_1^{51,61}$, T_2^{51}, and $NOE^{51,61}$. Employing T_2 in the analysis resulted in a $D_\parallel/D_\perp$ ratio (1.25) in good agreement with those of previous studies (Tjandra et al., 1995; Lee et al., 1997). Interestingly, when $T_{1\rho}^{61}$ data were substituted for T_2^{51} data, significant changes in the best fit θ and ϕ resulted, reflecting the differences that exist between these two data sets. When only T_1 and NOE data were employed, the obtained $D_\parallel/D_\perp$ ratio was determined to be 0.83, corresponding to diffusion consistent with an oblate shape as opposed to the prolate shape suggested by the result using T_2 data. In addition, the orientations of the principal axes are dramatically different [(θ, ϕ) = 1.31, 2.95 versus (θ, ϕ) = 0.56, 0.82 rad]. These discrepancies can be partially reconciled by the ~93° angle that the two principal axes make

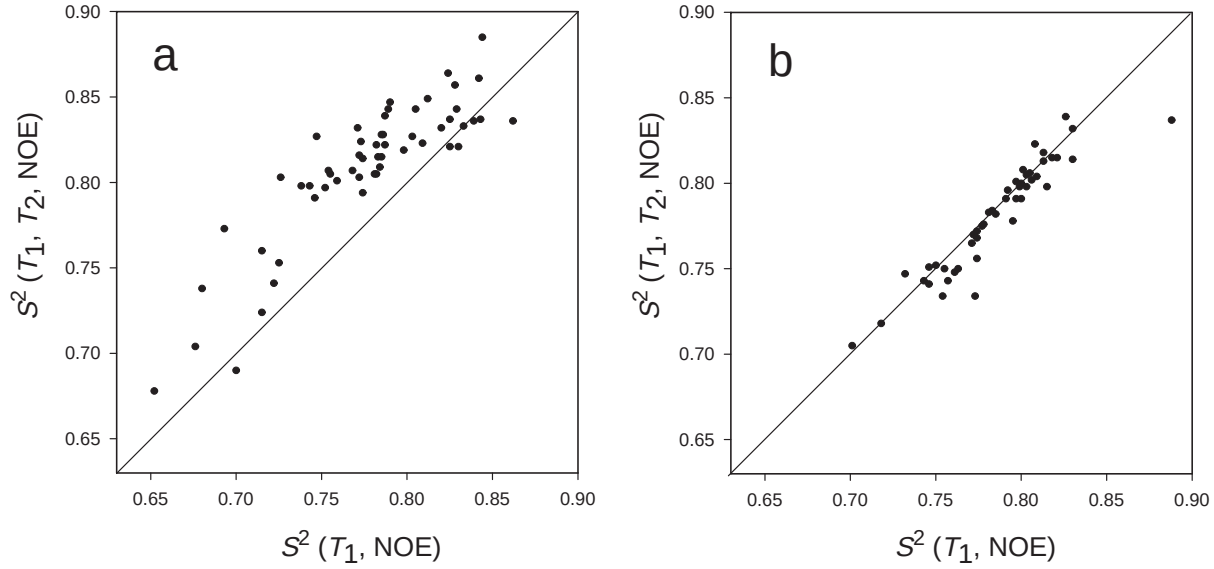

Figure 2. Correlation of the squares of the generalized order parameters (S^2) obtained from various fitting procedures and data combinations. (a) Three-parameter fits (S^2, τ_e, τ_m) were performed for a data combination including T_2 {$T_1^{51,61}$, T_2^{51}, NOE^{51,61}} and a data combination using only T_1 and NOE, {$T_1^{41,61}$, NOE^{51,61}}. $\Delta\sigma$ was fixed at -170 ppm. Residues 74–76 were excluded. (b) Four-parameter fits (S^2, τ_e, τ_m, $\Delta\sigma$) were performed with a data combination including T_2 {$T_1^{51,61,76}$, T_2^{51}, NOE^{51,61,76}} and one using only T_1 and NOE data, {$T_1^{51,61,76}$, NOE^{51,61,76}}. Flexible residues 8–12, 48,49, 62 and 74–76 were excluded.

with each other. It may be that in reality the ubiquitin diffusion tensor is completely non-symmetric, but the NMR data is not reliable enough to fit out such small anisotropies using data collected at the field strengths used here. If so, then when T_2 data is added to the T_1 and NOE data, the D_i would be slightly more consistent with a prolate rather than an oblate approximation. This is consistent with results from a test in which 5% random error was projected onto all T_2 values, a conservative error (i.e. perhaps underestimated) with the above considerations. The resultant axially symmetric diffusion tensor was ambiguous since 60% of the obtained tensors were prolate and 40% were oblate in the Monte Carlo simulations, and θ and ϕ varied widely. In a recent study, similar behavior was observed for cytochrome c_2 as a result of a fully anisotropic diffusion tensor (Blackledge et al., 1998). Indeed, from the components of the ubiquitin inertia tensor (1.00:0.90:0.64), one would expect ubiquitin, in detail, to tumble with completely non-symmetric anisotropy.

Conclusions

If general, the analysis presented here would seem to point to a potential explanation for much of the historical 25–30% discrepancy between τ_m values determined by fluorescence and NMR methods and place its origin in the use of T_2. It also suggests that, in the absence of $J(0)$ information, T_1 should be collected at the lowest possible field strength. This will aid in the determination of τ_m (Figure 1) as well as reduce the effects of uncertainty in the true ^{15}N CSA for model-free fitting. Using the unusually broad set of relaxation parameters obtained, we have determined a value of -170 ± 15 ppm for the breadth of the amide nitrogen chemical shift tensor. A second T_1 measurement should be made at higher field, which helps determine S^2, τ_e , and τ_m, and it can be measured with greater sensitivity and spectral resolution. If the true τ_m is at the T_1 minimum for a given field strength ($\omega_N\tau_m \sim 1$), that T_1 will be more effective at determining S^2 and τ_e, and the higher field T_1 should then constrain τ_m. At least one NOE measurement should be made to aid in the characterization of internal motions, and as always, it is important that the parameters are fitted from an experimentally overdetermined data set. Indeed, the fundamental inconsistency of the T_2 data that we

Table 3. Rotational diffusion tensor of ubiquitin at 25 °C[a]

	θ (rad)	ϕ (rad)	$D_\parallel/D_\perp$	D_{iso} ($\times 10^7$ s^{-1})	χ^2
Ubiquitin {T_1, NOE}[b]	1.31 (0.11)	2.95 (0.11)	0.82 (0.02)	3.85 (0.03)	118
Ubiquitin {T_1, T_2, NOE}[c]	0.56 (0.06)	0.82 (0.12)	1.25 (0.02)	3.53 (0.01)	105
Ubiquitin {T_1, $T_{1\rho}$, NOE}[d]	0.81 (0.05)	0.98 (0.05)	1.19 (0.01)	3.44 (0.01)	193
Ubiquitin[e]	0.71 (0.03)	0.81 (0.05)	1.15 (0.01)	4.01 (0.01)	638

[a] For 4 mM ^{15}N-labeled recombinant human ubiquitin in 90% H_2O/10% D_2O, 50 mM acetate-d_3, pH 5.0, and 0.02% NaN_3 at 25 °C. Parameters were fitted using the local diffusion approach (see text). Standard errors obtained from Monte Carlo simulations are given in parentheses.

[b] Fitted from $T_1^{41,51,61}$ and NOE^{51,61} data.

[c] Fitted from $T_1^{51,61}$, T_2^{51}, and NOE^{51,61} data. For ~7% of the Monte Carlo simulations, $D_\parallel/D_\perp$ was less than 1.0. These were excluded from average and error calculations.

[d] Fitted from $T_1^{51,61}$, $T_{1\rho}^{61}$, and NOE^{51,61} data.

[e] Taken from Tjandra et al. (1995) and Lee et al. (1997) for ubiquitin at 1.5 mM.

have observed would not have been detected without availability of the extensive T_1 and NOE parameters.

Here we have opted to determine τ_m using the local site approach, but for most cases the globally linked approach (Dellwo and Wand, 1989) will give equivalent results unless significant tumbling anisotropy exists (Schurr et al., 1994). On the other hand, one should be careful when using extremely high-field data (> 61 MHz, for the case of ^{15}N) if the true CSA is not known to high accuracy since this quantity begins to affect fitted parameters. This would not be a problem if the uncertainty is accounted for in the Monte Carlo simulations. It now appears that −170 ppm should be used as the consensus value about which a Monte Carlo analysis can be centered.

If T_2 or $T_{1\rho}$ data must be used (e.g. for $\tau_m \geq 7$ ns in the case of ^{15}N relaxation), it may be wise to use these data only for determining τ_m, realizing that τ_m may be overestimated. Once τ_m is established, the T_2 data may be discarded, and the T_1 and NOE data should be sufficient to fit the internal parameters. The inconsistencies in T_2 will then be distributed uniformly over all residues, allowing reliable comparison of S^2 and τ_e between different residues, even if conformational exchange is present. We have found that although this procedure may have rather small, generally inflating effects on the resultant S^2 values for a given form of $J(\omega)$, it can have a substantial reducing effect on large χ^2 values arising from spurious T_2 errors in specific residues (e.g. from resonance offset effects), hence affecting model selection.

For ^{13}C data at typical field strengths (9–17 T), T_2s will more commonly be necessary for precise determination of τ_m values of proteins since the Larmor frequency is much larger than that for ^{15}N. For the same reason, i.e. increased contribution to T_1 from internal motion, ignoring internal motions becomes a poor approximation when ^{13}C is used. Therefore, the most reliable method should be to minimize either Equation 2 for local τ_ms or a global error function (Dellwo and Wand, 1989) using T_1, {^{1}H}-^{13}C NOE, and T_2 data, if necessary. ^{13}C T_1/T_2 ratios should be avoided, as these lead to increased underestimation of τ_m as the true correlation time increases.

Acknowledgements

We are indebted to Brian Volkman for assistance collecting 9.4 T relaxation data at the National NMR Facility at Madison and to Ramona Bieber Urbauer for preparation of ubiquitin. We also gratefully acknowledge Mikael Akke and Art Palmer for sending us their implementation of the $R_{1\rho}$-R_1 experiment. This research was supported by NIH grant GM35940 and ARO grant DAAH04–96–1–0312. A.L.L. is a recipient of an NIH postdoctoral fellowship (GM18114). This study made use of the National Nuclear Magnetic Resonance Facility at Madison (NMRFAM) which is supported by NIH grants RR02301, RR02781, and RR08438, NSF grants DMB-8415048 and BIR-9214394, the University of Wisconsin, and the U.S. Department of Agriculture.

References

Abragam, A. (1961) *Principles of Nuclear Magnetism*, Oxford University Press, Oxford, U.K.

Akke, M. and Palmer, A.G. (1996) *J. Am. Chem. Soc.*, **118**, 911–912.

Akke, M., Liu, J., Cavanagh, J., Erickson, H.P. and Palmer, A.G. (1998) *Nat. Struct. Biol.*, **5**, 55–59.
Barbato, G., Ikura, M., Kay, L.E., Pastor, R.W. and Bax, A. (1992) *Biochemistry*, **31**, 5269–5278.
Blackledge, M., Cordier, F., Dosset, P. and Marion, D. (1998) *J. Am. Chem. Soc.*, **120**, 4538–4539.
Brüschweiler, R., Liao, X. and Wright, P.E. (1995) *Science*, **268**, 886–889.
Buck, M., Boyd, J., Redfield, C., MacKenzie, D.A., Jeenes, D.J., Archer, D.B. and Dobson, C.M. (1995) *Biochemistry*, **34**, 4041–4055.
Cantor, C.R. and Schimmel, P.R. (1980) *Biophysical Chemistry*, W.H. Freeman and Company, New York, NY.
Cordier, F., Brutscher, B. and Marion, D. (1996) *J. Biomol. NMR*, **7**, 163–168.
Dellwo, M.J. and Wand, A.J. (1989) *J. Am. Chem. Soc.*, **111**, 4571–4578.
Dellwo, M.J. and Wand, A.J. (1991) *J. Magn. Reson.*, **91**, 505–516.
Di Stefano, D.L. and Wand, A.J. (1987) *Biochemistry*, **26**, 7272–7281.
Deverell, C., Morgan, R.E. and Strange, J.H. (1970) *Mol. Phys.*, **18**, 553–559.
Dubin, S.B., Clark, N.A. and Benedek, G.B. (1971) *J. Chem. Phys.*, **14**, 5138–5164.
Farrow, N.A., Muhandiram, R., Singer, A.U., Pascal, S.M., Kay, C.M., Gish, G., Shoelson, S.E., Pawson, T., Forman-Kay, J.D. and Kay, L.E. (1994) *Biochemistry*, **33**, 5984–6003.
Frauenfelder, H. and Wolynes, P.G. (1985) *Science*, **229**, 337–345.
Frauenfelder, H., Sligar, S.G. and Wolynes, P.G. (1991) *Science*, **254**, 1598–1603.
Goldman, M. (1984) *J. Magn. Reson.*, **60**, 437–452.
Hiyama, Y., Niu, C.H., Silverton, J.V., Bavoso, A. and Torchia, D.A. (1988) *J. Am. Chem. Soc.*, **110**, 2378–2383.
Kay, L.E., Torchia, D.A. and Bax, A. (1989) *Biochemistry*, **28**, 8972–8979.
Kemple, M.D., Yuan, P., Nollet, K.E., Fuchs, J.A., Silva, N. and Prendergast, F.G. (1994) *Biophys. J.*, **66**, 2111–2126.
Korzhnev, D.M., Orekhov, V.Y. and Arseniev, A.S. (1997) *J. Magn. Reson.*, **127**, 184–191.
Kowalewski, J. and Werbelow, L. (1997) *J. Magn. Reson.*, **128**, 144–148.
Lee, L.K., Rance, M., Chazin, W.J. and Palmer, A.G. (1997) *J. Biomol. NMR*, **9**, 287–298.
Lefevre, J.F., Dayie, K.T., Peng, J.W. and Wagner, G. (1996) *Biochemistry*, **35**, 2674–2686.
Lipari, G. and Szabo, A. (1982a) *J. Am. Chem. Soc.*, **104**, 4546–4559.
Lipari, G. and Szabo, A. (1982b) *J. Am. Chem. Soc.*, **104**, 4559–4570.
Nirmala, N.R. and Wagner, G. (1988) *J. Am. Chem. Soc.*, **110**, 7557–7558.
Oas, T.G., Hartzell, C.J., Dahlquist, F.W. and Drobny, G.P. (1987) *J. Am. Chem. Soc.*, **110**, 2378–2383.
Ottiger, M., Tjandra, N. and Bax, A. (1997) *J. Am. Chem. Soc.*, **119**, 9825–9830.
Palmer, A.G., Skelton, N.J., Chazin, W.J., Wright, P.E. and Rance, M. (1992) *Mol. Phys.*, **75**, 699–711.
Palmer, A.G., Hochstrasser, R.A., Millar, D.P., Rance, M. and Wright, P.E. (1993) *J. Am. Chem. Soc.*, **115**, 6333–6345.
Palmer, A.G., Williams, J. and McDermott, A. (1996) *J. Phys. Chem.*, **100**, 13293–13310.
Peng, J.W., Thanabal, V. and Wagner, G. (1991) *J. Magn. Reson.*, **94**, 82–100.
Peng, J.W. and Wagner, G. (1994) *Methods Enzymol.*, **239**, 563–596.
Press, W.H., Teukolsky, S.A., Vetterling, W.T. and Flannery, B.P. (1992) *Numerical Recipes in Fortran 77: The Art of Scientific Computing*, Cambridge University Press, Cambridge, U.K.
Raiford, D.S., Fisk, C.L. and Becker, E.D. (1979) *Anal. Chem.*, **51**, 2050–2051.
Ross, A., Czisch, M. and King, G.C. (1997) *J. Magn. Reson.*, **124**, 355–365.
Schurr, J.M., Babcock, H.P. and Fujimoto, B.S. (1994) *J. Magn. Reson.*, **B105**, 211–224.
Schneider, D.M., Dellwo, M.J. and Wand, A.J. (1992) *Biochemistry*, **31**, 3645–3652.
Simbrunner, J. and Stollberger, R. (1995) *J. Magn. Reson.*, **B109**, 301–309.
Sklenar, V., Torchia, D. and Bax, A. (1987) *J. Magn. Reson.*, **73**, 375–379.
Tanford, C. (1961) *Physical Chemistry of Macromolecules*, John Wiley and Sons, Inc., New York, NY.
Taylor, J.R. (1982) *An Introduction to Error Analysis*, University Science Books, Mill Valley.
Tjandra, N., Feller, S.E., Pastor, R.W. and Bax, A. (1995) *J. Am. Chem. Soc.*, **117**, 12562–12566.
Tjandra, N., Szabo, A. and Bax, A. (1996a) *J. Am. Chem. Soc.*, **118**, 6986–6991.
Tjandra, N., Wingfield, P., Stahl, S. and Bax, A. (1996b) *J. Biomol. NMR*, **8**, 273–284.
Wand, A.J., Urbauer, J.L., McEvoy, R.P. and Bieber, R.J. (1996) *Biochemistry*, **35**, 6116–6125.
Wang, J. and Wolynes, P.G. (1993) *Chem. Phys. Lett.*, **212**, 427–433.
Zeng, L., Fischer, M.W.F. and Zuiderweg, E.R.P. (1996) *J. Biomol. NMR*, **7**, 157–162.
Zhou, H.-X. and Zwanzig, R. (1991) *J. Chem. Phys.*, **94**, 6147–6152.